11.4 STUDY OF CLEAR SKY, LOW-LEVEL ATMOSPHERIC TEMPERATURE INVERSIONS USING SATELLITE DATA

Yinghui Liu[1]* and Jeffrey R. Key[2]
[1]Cooperative Institute for Meteorological Satellite Studies
University of Wisconsin-Madison, Madison, Wisconsin
[2]Office of Research and Applications, NOAA/NESDIS
Madison, Wisconsin

1. ABSTRACT

The near-surface atmosphere of the polar regions is characterized by temperature inversions throughout most of the year. However, radiosonde data are sparse, and numerical weather prediction models have relatively poor vertical resolution for boundary layer studies. A method is developed for detecting and estimating the characteristics of clear sky, low-level temperature inversions using the Moderate Resolution Imaging Spectroradiometer (MODIS). The method is based on an empirical relationship between the inversion strength, defined as the temperature difference across the inversion, or height, defined as the altitude difference, and the difference between brightness temperatures in the 7.2 m water vapor and 11 m infrared window bands. Results indicate that inversion strength can be estimated with a root-mean-square error (RMSE) of 2-3^{o}C. Inversion height can be estimated with a RMSE of 130-250 m.

2. INTRODUCTION

Low-level atmospheric temperature inversions are ubiquitous at high latitudes during the low-sun and dark periods of the year. Temperature differences across inversions range from a few degrees to more than 30^{o}C, depending on the season and altitude, and their height are commonly lower than 700 hPa. Inversions are associated with extremely stable, persistent conditions that decouple the surface from the lower troposphere above the inversion. They may result from radiative cooling, warm air advection over a cooler surface layer, subsidence, surface melt, and topography.

Previous studies of Arctic and Antarctic temperature inversions were based on radiosonde data (cf., Kahl, 1990; Serreze et al., 1992; Bradley et al., 1992; Bradley et al, 1993; Walden et al., 1996; Stone and Kahl, 1991). However, radiosonde data are sparsely distributed across the Arctic and Antarctic, and therefore provide little information on the spatial distribution of temperature inversions. Can satellite data be used to observe temperature inversion structure? There are operational atmospheric sounders on polar-orbiting satellites that provide reasonably accurate temperature profiles overall, but retrieval methods are generally not optimized for the lower troposphere.

* *Corresponding author address*: Yinghui Liu, 1225 West Dayton St., Madison, WI 53706; e-mail: yinghuil@ssec.wisc.edu.

In this paper we extend the work of Ackerman (1996), who found that large negative brightness temperature differences between infrared window and water vapor channels of the High Resolution Infrared Sounder (HIRS) over Antarctica were associated with atmospheric temperature inversions. Here we use spectral bands that measure water vapor and carbon dioxide closer to the surface than the 6.7 m band used by Ackerman (1996), and are therefore able to detect weaker and shallower inversions. Empirical equations for estimating the inversion strength, defined as the temperature difference between the surface and the top of the inversion, and height, defined as the altitude of the maximum inversion temperature above the surface, are presented. The methods are then applied to a sample of MODIS scenes in both polar regions, and the estimated inversion characteristics are compared to those from a numerical model and from another retrieval method. Results are restricted to clear sky conditions because thermal satellite sensors cannot measure surface or near-surface conditions under cloud cover.

3. DATA

The soundings data used in this study are from four Antarctic and eight Arctic meteorological stations (Figure 1) for the period October 2000 to March 2002. The atmospheric sounding data for South Pole was obtained from the Antarctic Meteorological Research Center at University of Wisconsin-Madison. This data is high-resolution radiosonde data, with measurements taken at intervals of approximately 3 seconds. The standard resolution data for the other stations were obtained from the National Oceanic and Atmospheric Administration's (NOAA) Forecast System Laboratory. The radiosonde data are twice daily at 0000 and 1200 UTC. Pressure, height, temperature, and dew point temperature are available for each sounding. Of the 12 stations, South Pole has a very high surface elevation (2830 m); the others have surface elevations less than 250 m. As will be demonstrated below, surface elevation plays an important role in the development of the temperature inversion retrieval methods. Therefore, all data are separated into two groups: the high surface elevation data from South Pole, and the low surface elevation data from the other 11 weather stations.

The Moderate Resolution Imaging Spectroradiometer (MODIS) on-board the National Aeronautics and Space Administration's (NASA) Terra and Aqua polar-orbiting satellites provides global observations of the earth's land, oceans, and atmosphere in the visible and infrared regions of the

spectrum at 36 wavelengths from 0.4 to 14.5 m. The MODIS data product used in this study, called "MOD07_L2", is generated daily at 5 km spatial resolution. It provides brightness temperatures for 12 MODIS infrared channels (numbers 24-36, 4.5-14.3 m) and retrieved temperature profiles at 20 pressure levels under clear conditions. The 1 km "MOD35_L2" cloud mask product is used to determine whether a location is cloudy or clear. The MODIS data were obtained from the NASA Goddard Space Flight Center Distributed Active Archive Center (DAAC).

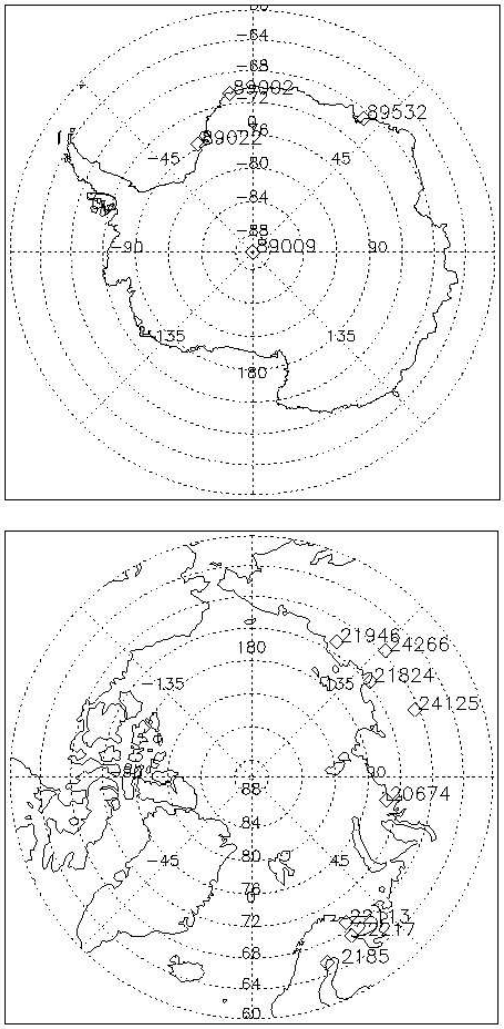

Fig. 1. Locations of the Antarctic (top) and Arctic (bottom) weather stations used in this study.

Only clear shy cases are examined, as determined by the cloud mask in the MOD07_L2 dataset. For each clear sky radiosonde profile, the closest MODIS 5 km pixel in time and space is used. In all there are 137 collocated radiosonde-MODIS samples for the high surface elevation group and 255 collocated samples for the low surface elevation group. The samples cover all seasons.

Temperature profiles from the National Centers for Environmental Prediction/National Center for Atmospheric Research (NCEP/NCAR) Reanalysis project are used for comparison with MODIS retrievals. The NCEP reanalysis data was obtained from NOAA's Climate Diagnostics Center. The data provides air temperature and geopotential height at 17 pressure levels (1000, 925, 850, 700, 600, 500, 400, 300, 250, 200, 150, 100, 70, 50, 30, 20, 10 hPa) four times per day at 0, 6, 12, and 18 UTC. The spatial resolution of the data is 2.5-degree latitude $\times$ 2.5-degree longitude.

4. THEORETICAL BASIS

In this study we are concerned only with clear sky temperature inversions in the lower troposphere. Inversions are assumed to have their base at the surface, so the base height is the meteorological station elevation. The top of the inversion is the height with the maximum temperature measurement in the radiosonde profile below 400 hPa. If the maximum temperature is within an isothermal layer, the top of the inversion is defined as the height at the top of the isothermal layer. The inversion strength is defined as the difference between the surface temperature and the temperature of the inversion top. The temperature inversion height is defined as the altitude difference between the surface and the temperature inversion top. Figure 2 shows a typical temperature profile with a temperature inversion.

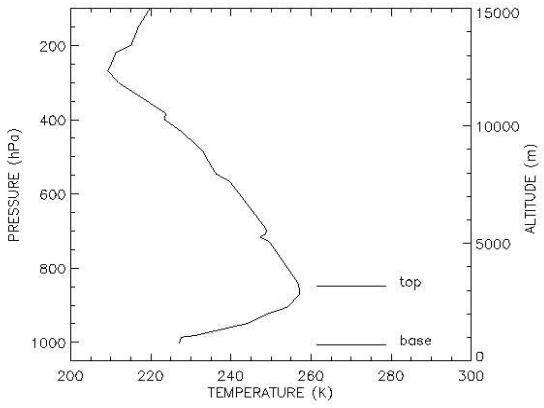

Fig. 2. Temperature profile measured at Verhojansk, Russia, 1200 UTC on 3 December 2001. Inversion top and base are indicated.

Upwelling thermal radiation measured by MODIS is a function of the atmospheric transmittance at a given wavelength and the atmospheric temperature. The channel weighting function, which is the derivative of transmittance with respect to pressure, describes the degree to which radiation emitted at various vertical

levels contributes to the upwelling radiance. Figure 3 gives the relative weighting functions for MODIS channels 27 (6.7 m), 28 (7.2 m), 31 (11 m), 33 (13.3 m) and 34 (13.6 m), calculated for the U.S. standard atmosphere. The peaks of the weighting functions for the 6.7 m, 7.2 m, 11 m, 13.3 m and 13.6 m channels are approximately 500 hPa, 750 hPa, the surface, 950 hPa, and 900 hPa, respectively. Because the weighting functions are broad and represent an average radiance contribution from a layer, the measured brightness temperature is sensitive to a relatively thick layer.

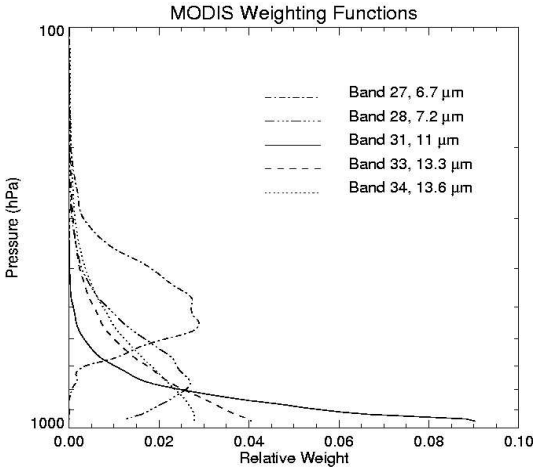

Fig. 3. Weighting functions for the MODIS bands at 6.7 m, 7.2 m, 11 m, 13.3 m, and 13.6 m.

As Figure 3 shows, the brightness temperature of the window channel at 11 m, BT_{11}, will be most sensitive to the temperature of the surface. The 7.2 µm water vapor channel brightness temperature, $BT_{7.2}$, is most sensitive to temperatures near 750 hPa. The magnitude of the brightness temperature difference (BTD) between the 7.2 m and 11 m channels, $BT_{7.2}$-BT_{11}, will therefore be proportional to the strength of temperature difference between the 750 hPa layer and the surface, which is related to the inversion strength. This should also be true for the two 13 m carbon dioxide channels. The 6.7 m water vapor band peaks near 500 hPa, so $BT_{6.7}$-BT_{11} can also provide information about inversion strength. In the Arctic and the low surface elevation areas of the Antarctic, the temperature inversion top is typically below 700 hPa (Serreze et al., 1992; Bradley et al., 1992), so $BT_{7.2}$-BT_{11} will better represent the inversion strength than will $BT_{6.7}$-BT_{11}. $BT_{7.2}$-BT_{11} is also more effective than $BT_{13.3}$-BT_{11} and $BT_{13.6}$-BT_{11} in providing information on inversion strength because the surface contribution is larger at 13.3 m and 13.6 m channels than at 7.2 m. On the Antarctic plateau where the surface pressure is typically 600-700 hPa, the peak of the 6.7 m and 7.2 m weighting functions are at the similar height, so both $BT_{7.2}$-BT_{11} and $BT_{6.7}$-BT_{11} can provide useful information on inversion strength.

The brightness temperature difference is not only the function of the temperature inversion strength, but also the inversion height. To illuminate the relationship between BTDs and both inversion strength and inversion height, the radiative transfer model *Streamer* (Key and Schweiger, 1998) is used to simulate MODIS brightness temperatures. Given different radiosonde temperature and humidity profiles, the model can simulate the brightness temperature at each MODIS infrared channel. Results for inversion strength indicate strong linear relationships for all channel pairs and both surface elevation categories. For high elevation surfaces the relationships for inversion height are weak, especially when the BTD is large. For low elevation surfaces the linear relationships are stronger. For both elevation categories, larger BTDs indicate greater inversion heights.

It appears that MODIS data can, in theory, be used to estimate inversion strength and inversion height. Are similar relationships apparent in the MODIS data? For high elevation conditions, the correlation coefficient between temperature inversion strength and $BT_{6.7}$-BT_{11}, $BT_{7.2}$-BT_{11}, $BT_{13.3}$-BT_{11} and $BT_{13.6}$-BT_{11} are 0.97, 0.98, 0.95 and 0.93, respectively. For high elevation conditions, the correlation coefficient between temperature inversion height and $BT_{6.7}$-BT_{11}, $BT_{7.2}$-BT_{11}, $BT_{13.3}$-BT_{11} and $BT_{13.6}$-BT_{11} are 0.89, 0.90, 0.88 and 0.87, respectively. The relationships are similar to those based on simulated brightness temperatures.

5. RETRIEVAL OF TEMPERATURE INVERSION STRENGTH AND HEIGHT

a) Temperature Inversion Detection

To estimate the inversion strength using MODIS infrared brightness temperature data under clear conditions, it is first necessary to determine if, in fact, an inversion is present. This step is separate from the retrieval of inversion characteristics because the relationship between BTD and inversion strength is poor for weak, shallow inversions. We therefore choose to eliminate such inversions from the analysis. Since each BTD pair increases with the increasing inversion strength, a threshold is chosen for each BTD pair to identify those conditions without inversions or with weak inversions. If the threshold is set too high, some inversions will be missed. If it is set too low, there will be some false inversion detections. There is no single threshold that can unambiguously identify inversions. For the $BT_{7.2}$-BT_{11} test, we set the threshold to –8 K, which means that $BT_{7.2}$-BT_{11} greater than –8 K indicates the presence of an inversion. In this study we use $BT_{6.7}$-BT_{11} as the inversion detection test, with a threshold of –20 K. For high surface elevation areas like the interior of Antarctica, $BT_{6.7}$-BT_{11} is always higher than –20 K, which indicates that temperature inversions are common year round. In the Arctic and low surface elevation areas of the Antarctic, some (but not all)

inversions with strengths between 0 and 10 degrees will be missed. Overall, more than 70% of the inversions will be detected with this threshold. Unfortunately, about 7% of the non-inversion cases will be identified as inversions.

b) Retrieval of Temperature Inversion Strength

After applying the simple inversion threshold test to the data and excluding inversions with strengths less than 2 K that were not eliminated by the threshold test, the relationship between the observed MODIS BTDs and the temperature inversion strength is more obvious. Of the 255 total samples, 135 meet these two requirements for low elevation surfaces. The new relationships between BTD and temperature inversion strength give correlation coefficients for $BT_{6.7}$-BT_{11}, $BT_{7.2}$-BT_{11}, $BT_{13.3}$-BT_{11} and $BT_{13.6}$-BT_{11} of 0.80, 0.86, 0.82 and 0.78, respectively. The relationships for high elevation surfaces are unchanged. For both high and low surface elevation conditions, the relationship between temperature inversion strength and $BT_{7.2}$-BT_{11} is stronger and with less variability. Therefore, $BT_{7.2}$-BT_{11} is used to retrieve the temperature inversion strength.

Statistical regression equations were formulated to quantify the relationship between temperature inversion strength and various combinations of MODIS infrared band brightness temperatures under both high surface and low surface conditions. For low elevation surfaces we use:

$$T = 32.2+0.84*(BT_{7.2}-BT_{11})-4.63*(BT_{11}-BT_{12}) \\ -0.081*BT_{11}+0.021*(BT_{7.2}-BT_{11})^2$$

where BT_{12} is the 12 m brightness temperature. The 11 m temperature is a proxy for the surface temperature, which is correlated with inversion strength. The BT_{11}-BT_{12} "split window" difference provides additional information on the column water vapor amount, which is also related to inversion strength. For high elevation surfaces the same terms are used but with different coefficients.

The accuracy of the retrieval is shown in the Figure 4, where the regression equations, which produce unbiased estimates, were applied to MODIS data co-located with radiosonde temperature profiles. The figures show that temperature inversion strength can be estimated with a root-mean-square error (RMSE) of 1.9 K for high elevation surfaces, and an RMSE of 3.2 K for low elevations. The correlation coefficients are 0.983 and 0.888, respectively. All temperature profiles are from land stations (though some are coastal), so the applicability of these equations over sea ice is not known. To test the stability of the equations, two-thirds of all the cases were randomly selected 1000 times with new regression coefficients determined for each, and with the equation applied to the remaining one-third of samples. The bias of the differences between the estimated inversion strengths from statistical equations and from 1000 sample regressions is 0.30 K for high surfaces and 0.20 K for low surfaces. The RMSE of the inversion strength differences (using statistical equations and the 1000 sample regression) is 0.38 K for high surfaces and 0.34 K for low surfaces. With differences between the regressions using the full dataset and the sample regression being close to zero, the results presented in Figure 4 would be similar if statistical equations were developed with an arbitrarily chosen subset of the data.

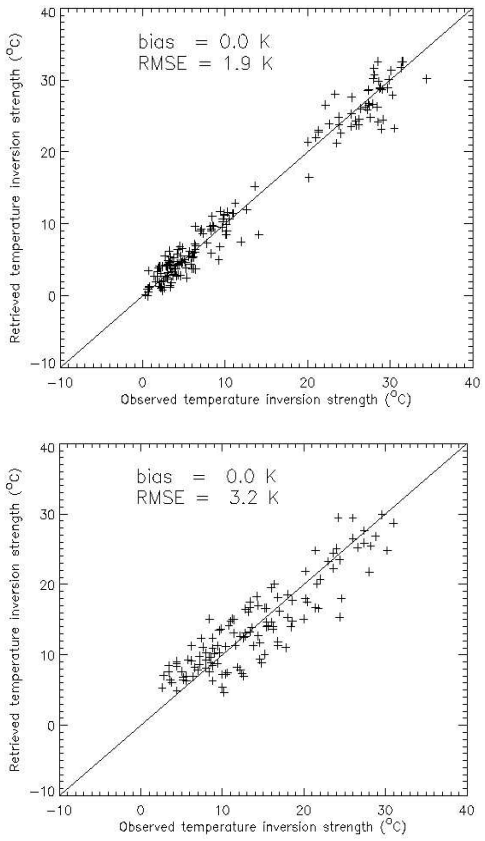

Fig. 4. Comparison of observed (radiosonde) inversion strength and retrieved (MODIS) inversion strength with high elevation surfaces (top) and low elevation surfaces (bottom). The bias and root-mean-square error (RMSE) are given.

c) Retrieval of Temperature Inversion Height

A similar approach can be used to estimate the inversion height. However, both the simulated and actual MODIS data indicate that the relationship between BTDs and temperature inversion height is not as strong as for the inversion strength. When $BT_{6.7}$-BT_{11} is larger than about 10 K, indicative of strong inversions, the relationship is weak. It was also found that when the maximum relative humidity in a profile is larger than 90%, there is no apparent linear relationship

between inversion height and BTD. So we impose a further restriction on the dataset, such that profiles with maximum relative humidities larger than 90% are excluded.

For low elevation surfaces the correlation coefficients for $BT_{6.7}$-BT_{11}, $BT_{7.2}$-BT_{11}, $BT_{13.3}$-BT_{11} and $BT_{13.6}$-BT_{11} are 0.69, 0.73, 0.72 and 0.67, respectively. As with inversion strength, there is a somewhat stronger relationship between temperature inversion height and $BT_{7.2}$-BT_{11} than for the other BTD pairs. Therefore, $BT_{7.2}$-BT_{11} is used to retrieve the temperature inversion height. For low elevation surfaces we use:

$$Z = 2001.5+38.9*(BT_{7.2}-BT_{11})-149.5*(BT_{11}-BT_{12}) -5.38*BT_{11}+0.09*(BT_{7.2}-BT_{11})^2 \quad (3)$$

For high elevation surfaces the regression is of the same form but with different coefficients.

The inversion height increases when $BT_{7.2}$-BT_{11} increases or BT_{11} decreases. The comparison of the retrieved inversion height and the observed inversion height is shown in Figure 5.

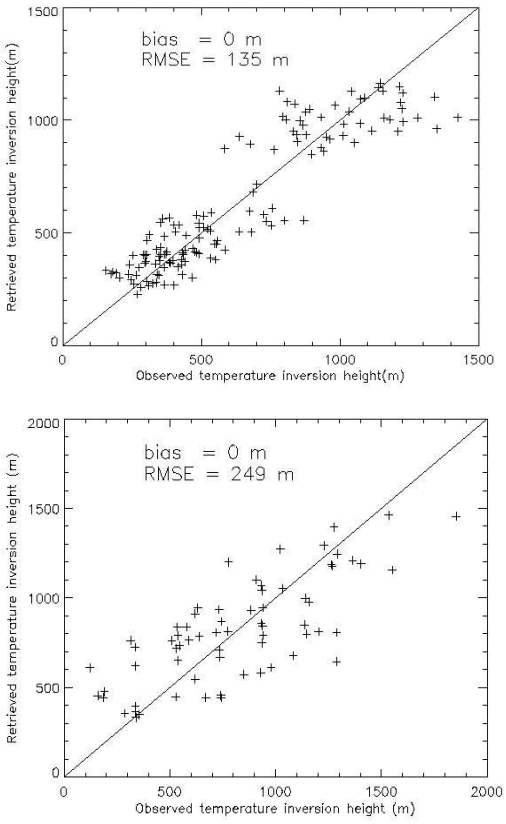

Fig. 5. Comparison of observed (radiosonde) inversion height and retrieved (MODIS) inversion height with high elevation surfaces (top) and low elevation surfaces (bottom). The bias and root-mean-square error (RMSE) are given.

d) Adjustment for Elevation

The radiosonde dataset used in this study includes 11 stations with elevations less than 250 m and one station with an elevation of 2800 m. What should be done for elevations between these two? Simulations with the radiative transfer model show that when the surface elevation increases, the BTD increases, but the BTD increases more for the data with lower inversion strengths. So, when the surface elevation is higher than 2800 m, the regression equation for the high surface elevation is used. When the surface elevation is lower than 250 m, the regression equation for the low surface elevation is used. For locations with elevations between 250 m and 2800 m, we use linear combination of the retrieved inversion strength for high and low surfaces, weighted by the fractional distance of the actual elevation between 250 m and 2800 m. The retrieval of the temperature inversion height uses the same method.

e) Error Sources

Error in the retrievals of inversion strength and height may originate from a variety of sources. First, radiosonde data for the lower elevation stations is of relatively low vertical resolution. Both the inversion temperature and height used as truth may be inaccurate as a result. This error can be as high as 0.50 K and 88 m. Second, inversion structure can differ significantly from the more ideal shape shown in Figure 2. Third, there is some uncertainty in the MODIS Cloud Mask product, which we use to identify clear sky pixels. Clouds strongly affect the BTDs, so cloud contamination is a potential problem.

6. APPLICATION AND COMPARISON TO OTHER DATASETS

An application of the methods presented above is shown in Figure 6 for inversion strength and Figure 7 for inversion height. Both figures give results for a single winter day over the Arctic and Antarctic. The images are composites of consecutive MOD07_L2 overpasses, subsampled to 10 km resolution. No results are given for cloudy areas (white). For the Arctic, inversion strength varies from 0 to 30 ^{o}C. In the coastal areas and the northern portions of the Greenland and Norwegian Seas, the inversion strength is low due to turbulent mixing over the open water. Inversion strength over the pack ice is higher, with values in the range 12-18 ^{o}C. Inversion strength generally increases inland due to stronger radiative cooling.

The spatial pattern of inversion height (Figure 7) is similar to that of inversion strength. It ranges from 0 to 1500 m over the Arctic, with a minimum some coastal areas and near the ice edge. The greatest inversion height and strength are found near the Yenisey River valley, Lena River valley, and Kolyma River valley in Russia and Siberia, where the cold air drainage associated with the strong wintertime Siberian High pressure cell result in strong temperature inversions

(Serreze et al. 1992). Over Greenland, the inversion strength and inversion depth are moderately large due to the strong surface radiative cooling.

The inversion strength over Antarctic Plateau is greater than that in Arctic, primarily due to the stronger high surface radiative cooling. Inversion strength and height increase with increasing surface elevation. The maximum inversion strength is near 40 ^{o}C, and maximum inversion height is approximately 1500 m.

Temperature inversion strength and inversion height can also be derived from the NCEP profile data. The inversion strength has a similar spatial distribution for both polar regions, with large inversion strengths over land and the interior pack ice and smaller values over coastal areas. However, the MODIS image provides more detailed and accurate (based on comparisons with radiosonde data) information. Overall, inversion strengths from MODIS are larger than those from NCEP. This is due in part to the low vertical and horizontal resolutions of the NCEP data, where there are only 7 pressure levels under 400 hPa in the NCEP data and the horizontal resolution is 2.5 x 2.5 degree latitude/longitude. A comparison with inversion heights from the NCEP data produced similar results.

The MODIS regression retrievals were also compared to inversion characteristics derived from the MOD07_L2 temperature profile product. The MOD07_L2 product uses a physical (as opposed to statistical) retrieval method to get the temperature profile at 20 pressure levels. It is also for clear skies only. The 20 pressure levels are 5, 10, 20, 30, 50, 70, 100, 150, 200, 250, 300, 400, 500, 620, 700, 780, 850, 920, 950, 1000 hPa. The inversion strengths from the MOD07_L2 product are biased low, and the bias increases for stronger inversions. As with the NCEP data, this is in part due to the relatively low vertical resolution.

7. CONCLUSIONS

A method for estimating the strength of low-level atmospheric temperature inversions using clear sky infrared data from the MODIS instrument has been presented. The method involves an empirical relationship between the inversion strength, defined as the temperature difference across the inversion, or height, defined as the altitude difference, and the difference between satellite-measured brightness temperatures in the 7.2 m water vapor and 11 m infrared window bands. Results with MODIS data from all seasons indicate that inversion strength can be estimated unbiasedly with a root-mean-square error (RMSE) of 2-3 ^{o}C. The method is more accurate for high elevation surfaces (1.9 K RMSE), characterized by stronger inversions, than for low elevation surfaces (3.2 K RMSE). Inversion height can be estimated with an RMSE of 130-250 m.

Satellite retrievals of inversion strength and inversion height can be used to validate, and potentially improve, the parameterization of energy transfer processes in climate models. Parameters based on the estimated inversion strength, inversion height, and the bulk boundary-layer wind shear may be useful for monitoring climate change. With MODIS, temperature inversions can be observed at a spatial resolution as high as one square kilometer and a temporal sampling of up to fourteen times per day, providing an opportunity for detailed studies of the spatial distribution and temporal evolution of the high-latitude boundary layer.

Acknowledgements: This work was supported by NASA contract NAS5-31367.

8. REFERENCES

Ackerman, S.A., 1996: Global satellite observations of negative brightness temperature differences between 11 and 6.7 µm, *J. Atmos. Sci.*, 53, 2803-2812.

Ackerman, S.A., K.I. Strabala, W.P. Menzel, R.A. Frey, C.C. Moeller, and L.E. Gumley, 1998: Discriminating clear sky from clouds with MODIS, *J. Geophys. Res.*, 98, 32,141-32,157.

Bradley,R.S., F.T. Keiming, and H.F. Diaz, 1992: Climatology of surface-based inversions in the North American Arctic, *J. Geophys. Res.*, 97, 15,699-15,712.

Bradley,R.S., F.T. Keiming, and H.F. Diaz, 1993: Recent changes in the North American Arctic boundary layer in winter, *J.Geophys. Res.*, 98, 8851-8858.

Kahl,J.D., 1990: Characteristics of the low-level temperature inversion along the Alaskan arctic coast. *Int. J. Climatol.*, 10, 537-548.

Key, J. and A.J. Schweiger, 1998: Tools for atmospheric radiative transfer: Streamer and FluxNet, *Computers and Geosciences*, 24(5), 443-451.

Serreze, M. C., J. D. Kahl and R. C. Schnell, 1992: Low-level temperature inversions of the Eurasian Arctic and comparisons with Soviet drifting stations, *J. Climate*,5, 615-630.

Stone, R.S., and J.D. Kahl, 1991: Variations in boundary layer properties associated with clouds and transient weather disturbances at the south pole during winter, *J. Geophys. Res.*, 96, 5137-5144.

Walden, V.P., A. Mahesh, and S.G. Warren, 1996: Comment on "Recent changes in the North American Arctic boundary layer in winter" by R.S. Bradley et al., *J.Geophys. Res.*, 101, 7127-7134.

W.Paul Menzel and Liam E. Gumley, 1998: "Modis Atmospheric Profile Retrieval Algorithm Theoretical Basis document" at http://modis_atmos.gsfc.gov/MOD07_L2/atbd.html.

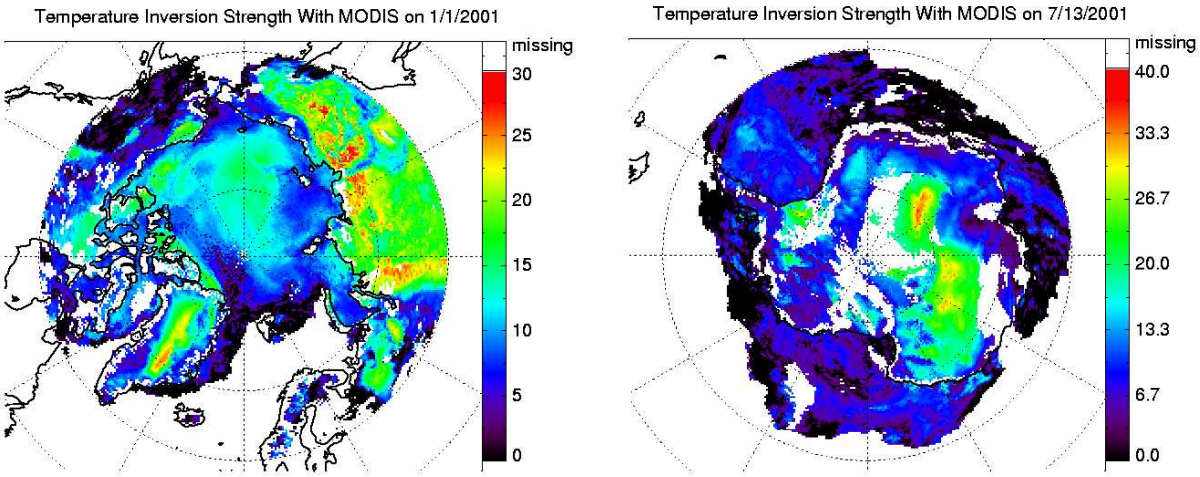

Fig. 6. Temperature inversion strength (^{o}C) estimated from MODIS over the Arctic (left) and Antarctic (right) on a single winter day for each hemisphere.

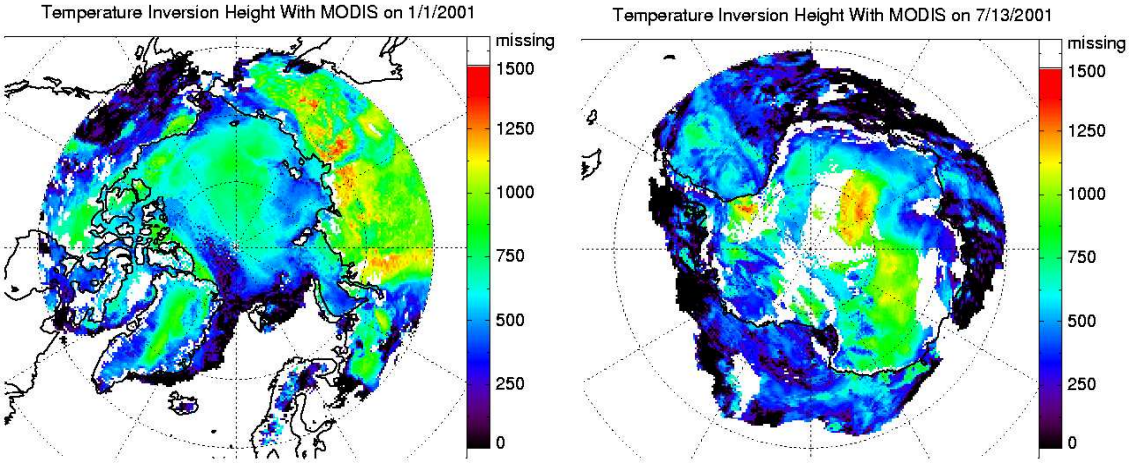

Fig. 7. Temperature inversion height (m) estimated from MODIS over the Arctic (left) and Antarctic (right) on a single winter day for each hemisphere.